Direct Observation of Microfibril Arrangement in a Single Native Cellulose Fiber by Microbeam Small-Angle X-ray Scattering

M. Müller,*,† C. Czihak,†,‡ G. Vogl,† P. Fratzl,†,|| H. Schober,‡ and C. Riekel§

Institut für Materialphysik der Universität Wien, Strudlhofgasse 4, A-1090 Wien, Austria, Institut Laue-Langevin, B.P. 156, F-38042 Grenoble Cedex 9, France, and European Synchrotron Radiation Facility, B.P. 220, F-38043 Grenoble Cedex 9, France

Received January 5, 1998; Revised Manuscript Received March 16, 1998

ABSTRACT: The arrangement of the crystalline cellulose microfibrils in native flax fibers was studied by means of position-resolved microbeam X-ray small-angle scattering (μSAXS) at the ESRF. The nearly perfect alignment of the microfibrils parallel to the fiber axis could for the first time be determined directly on a single fiber; a tilt angle distribution with a mean hwhm of 3.5° was measured. The lateral organization (i.e., diameter and mean distance) of the microfibrils showed no significant variation across the fiber on a length scale of 4 μm (beam size at sample position). The advantages of the μSAXS technique are discussed by comparing it to a conventional SAXS experiment on flax fibers.

1. Introduction

Cellulose is the most abundant biopolymer since it is used as a structural material by plants (and also some animals). The function of cellulose being the main component of cell walls is closely related to its hierarchical structure.[1] On the lowest, i.e., the molecular level cellulose can be regarded as an unbranched polymer consisting of $\beta(1\rightarrow4)$ linked glucose residues. These cellulose chains form small crystallites via van der Waals and hydrogen bonding. They are called *cellulose microfibrils*. In native cellulose two different crystal structures (cellulose Iα and Iβ) occur.[2] Part of the cellulose remains disordered and may as well be called amorphous. Concerning the *supermolecular* level—which has been subject to a large number of investigations during the last 50 years—differences in size and arrangement of the microfibrils show up between different organisms. E.g., the mean diameter of the microfibrils varies from 25 (spruce, *Picea abies*[3]) to 200 Å (*Valonia ventricosa*[4]), and in the latter (a monocellular green alga) an alignment of the $(\bar{1}10)$ planes (we refer to the unit cell of Woodcock et al.[5]) of the microfibrils with respect to the surface of the cell wall was observed.[4] The local aspects of the cellulose microfibrils' sizes and orientations are supposed to be closely related to the functional properties of different cell walls.

Many questions about the detailed supermolecular structure of cellulose still remain open. This is mainly due to the number of limitations imposed by the structural probes. Electron diffraction and electron microscopy are local probes but require an extensive treatment of the sample (embedding into resin, sectioning, staining or contrasting) which may introduce artifacts.[4,6] Furthermore, electron beams are known to cause beam damage in biological materials.[7] X-ray scattering solves these problems, however, conventional techniques (small- and wide-angle X-ray scattering, SAXS/WAXS[3,8−11]) cannot be used to study the organization of the microfibrils in single fibers or cell walls.

The aim of this article is to show that local area SAXS with beam sizes of a few micrometers (μSAXS) opens up a new window for position-resolved studies of biomaterials like cellulose. In the present study we chose to investigate fibers from the sclerenchyma support tissue of flax stems since we have already obtained conventional SAXS data on bundles of identical fibers.[12] In native flax stems, the fibers are organized in bundles located near the surface. Their diameters range from 10 to 30 μm, and they display polygonal to circular cross-sectional shapes.[6] Fiber cells have a very thick secondary cell wall and a small lumen. As the function of fibrous sclerenchyma is to support plant stems by rigidity and strength, the cell walls of fiber cells are (1) impregnated with lignin and (2) the cellulose microfibrils are aligned parallel to the fiber axis. The details of the preparation will be described below, followed by a presentation of experimental setup, results, and conclusions.

2. Sample

The fibers were extracted from flax stems by the commonly used retting process. With this treatment most of the "glue" connecting the fibers is removed by biological−chemical degradation. As the macroscopic fibers normally are an aggregate of several single fibers (see electron micrograph in Figure 1) the samples had to be prepared using a stereomicroscope. Once a single straight fiber—with a diameter of ≈20 μm—had been extracted, it was glued on both ends with super glue across the hole of a metal ring (diameter 4 mm).

It is known that the scattering contrast between disordered and crystalline parts of native cellulose samples is weak, but it may be enhanced by swelling the fiber in water:[8] The water can only access the amorphous regions and reduces their electron density by swelling. The crystalline microfibrils remain unchanged. Therefore, the flax fibers were allowed to

* To whom correspondance should be addressed (e-mail: mmueller@esrf.fr). Present address: European Synchrotron Radiation Facility.
† Institut für Materialphysik der Universität Wien.
‡ Institut Laue-Langevin.
|| Now at: Erich Schmid Institute of the Austrian Academy of Sciences and University of Leoben, Jahnstr. 12, A-8700 Leoben, Austria.
§ European Synchrotron Radiation Facility.

S0024-9297(98)00004-7 CCC: $15.00
Published on Web 05/28/1998

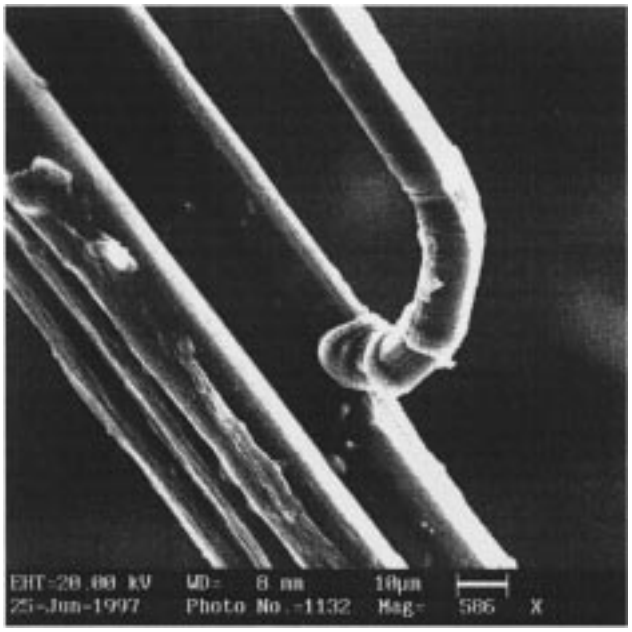

Figure 1. Electron micrograph of an aggregate of flax fibers. It shows the remaining glue of the intercellular binding of flax fibers. In the narrow (rightmost) fiber, typical dislocations ("kinks") are observed.

swell in water. For the experiment, they were taken out of the water but a water droplet was applied to the metal ring. During the relatively short measuring times (see the following section) the fibers could be kept wet in this way.

3. Experimental Details

In the present experiment on beamline ID13 (Microfocus) at the European Synchrotron Radiation Facility (ESRF), X-rays of 13 keV (wavelength 0.96 Å) were used. The monochromatic beam is focussed by an ellipsoidal mirror and further collimated with a glass capillary to a beam size of 2 μm fwhm diameter. The beam divergence is defined by the glass capillary to ≈2.3 mrad. At the exit of the capillary, a guard aperture is placed to reduce scattering coming from the capillary exit well. The sample position was 2 mm away from the aperture, resulting in a flux at the sample of $>10^{10}$ ph/s and a beam size of ≈ 4 μm (fwhm) in diameter. More details about the beamline setup may be found in a publication by Riekel et al.[13] The path between the sample and the detector mounted at a distance of 1100 mm was evacuated to reduce air scattering. Both beam stop and CCD detector[13] (surface 100×75 mm^2, pixel size 126×126 μm^2, with intensifier stage and video-readout) were placed directly at the exit window of the evacuated tube. In this setup, the accessible range of the wave vector transfer is 0.033 Å$^{-1} \le Q \le 0.203$ Å^{-1}. For angle calibration of the detector, a silver behenate sample was used.[14]

The metal ring with the fixed single fiber (see Sample section) was mounted on a goniometer head. The fiber axis was pre-aligned optically. The goniometer head plus sample were placed on a high-precision *x*/*y* stage. Here, the fiber was positioned in the center of a high-resolution microscope with a precisely known offset to the X-ray beam. Translation of a specific feature into the beam was accurate to chart 1 μm as shown by monitoring the cellulose 200 reflection.[5]

With this calibration, it was possible to scan across a single fiber (i.e., perpendicular to the fiber axis). The fiber was scanned in steps of 2 μm in a range of ± 30 μm with respect to the fiber center. For the present experiments, 400 frames of 40 ms each were accumulated at every position. Beam damage turned out to be a problem, as already pointed out by other authors investigating chemically similar materials (starch).[15,16] Possible solutions are cooling of the sample—associated with considerable instrumental efforts—or the use of faster and more sensitive detectors. Both options are under investigation. In our experiment, some fibers were even broken before the scan was completed. However, the small-angle pattern on a single point did not show any variation with time. The set of data presented in this work is complete in the sense that there was a small-angle signal for the full width of the fiber as determined in the optical microscope. However, also this specific fiber was found to be cut into two parts after the scan.

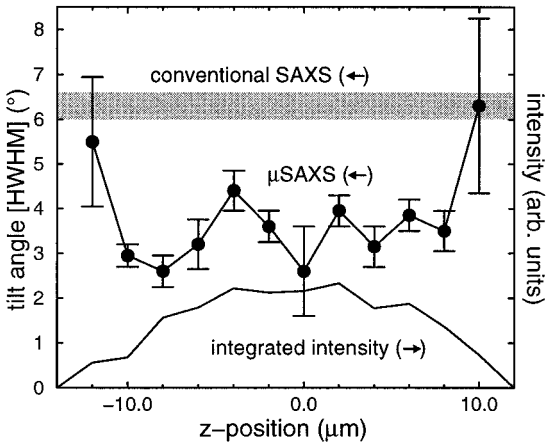

Figure 2. Position (z) dependence of integrated scattering intensity (solid line in lower part) and microfibril misalignment determined from the streak widths (hwhm) in the two-dimensional μSAXS patterns (full circles). For comparison, the misalignment measured in a conventional SAXS experiment[11] (averaged over a bundle of fibers) is also displayed (the shaded area also visualizes the error bars).

In addition to the μSAXS experiment, conventional measurements on bundles of dry and wet flax fibers were carried out, for comparison, at a laboratory X-ray source.[12] The corresponding experimental setup is described elsewhere.[3]

Data visualization and analysis were performed with the software package FIT2D.[17] The raw data were first background-corrected and afterwards integrated over the azimuth angle in order to obtain the spherically averaged intensity.[18] This scattering curve $\bar{I}(Q)$ is used in the further analysis.

4. Results and Discussion

In the transverse scan described above a SAXS signal was obtained in the position (z) range -12 μm $\le z \le$ $+10$ μm. The lower part of Figure 2 shows the integrated scattered intensity (full line). It is weaker towards the fiber edges, as one would expect. Accounting for the position resolution of ≈4 μm, the fiber diameter is determined to approximately 20 μm, thus, in good agreement with optical microscopy.

An example for a two-dimensional SAXS pattern (at position $z = -4$ μm) is shown in Figure 3. The fiber is oriented horizontally, and a small-angle intensity streak appears in vertical (equatorial) direction. This anisotropic SAXS pattern from cellulose fibers is well-known. It indicates the presence of scattering density fluctuations in the equatorial plane on a length scale of 10 Å. This contrast can be attributed to the different electron densities of crystalline cellulose microfibrils and less dense disordered material. No long-spacing Bragg reflections at small angles in equatorial or in meridional direction are observed. This is an indication for a nonperiodic microfibril arrangement in the cross section and along the fiber axis, respectively, as known from investigations of a number of native cellulose fibers. In contrast, such reflections were previously found in SAXS patterns of regenerated cellulose II fibers.[19,20]

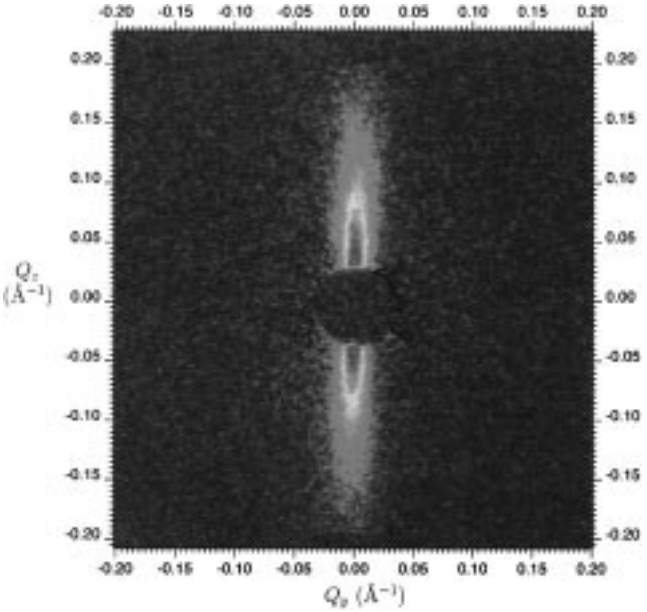

Figure 3. Two-dimensional μSAXS pattern of a horizontally oriented single flax fiber in the water-swollen state. The intensity (after background correction) is displayed on a pseudo gray scale. (The pattern was obtained at the position $z = -4$ μm on the fiber.)

4.1. Distribution of Microfibrillar Angles. The width of the intensity streak in Figure 3 depends linearly on the wave vector transfer in the z direction, Q_z. At this particular position, the regression slope of the streak widths (fwhm) as a function of Q_z corresponds to 8.8(9)°, thus, to a tilt angle of ±4.4° (hwhm). The linear increase corresponds directly to a misalignment of the microfibrils inside the fiber since the macroscopic fiber itself is straight on the scale of the beam size (i.e., a few microns). Similar data to those presented in Figure 3 were obtained at all positions on the fiber (for integral intensity, refer to the lower part of Figure 2). They were all analyzed in the manner described above. The resulting tilt angles with respect to the macroscopic fiber direction are displayed in the upper part of Figure 2 (filled circles). Except for the very edge of the fiber (i.e, $z = -12$ μm and $z = +10$ μm), the values are randomly distributed around 3.5°. The data from the edges display both larger tilt angles and errors. There are two possible reasons for this effect: (1) The statistics of the data are worse (see integrated intensity in Figure 2). (2) There might be an additional signal arising from refraction effects at the fiber edge;[21] this may change the shape of the SAXS signal. In conclusion, in view of the present data there is no evidence for a difference in microfibril orientation at fiber skin and core on a length scale of a few microns.

Hence, one can conclude on a nearly perfect orientation of the cellulose microfibrils parallel to the fiber axis for the whole cross section, with an average tilt of ±3.5° (hwhm). This angle is considerably smaller than conventionally determined average tilts. In our conventional SAXS experiment[12] with a bundle of wet flax fibers—aligned as well as possible—a mean tilt angle of ±6.3° (hwhm) was obtained (shaded area in Figure 2). Since a slight misalignment of the individual macroscopic fibers with respect to each other is obviously impossible to avoid, the μSAXS technique is required to directly obtain the distribution of microfibrillar tilt angles within a single macroscopic fiber.

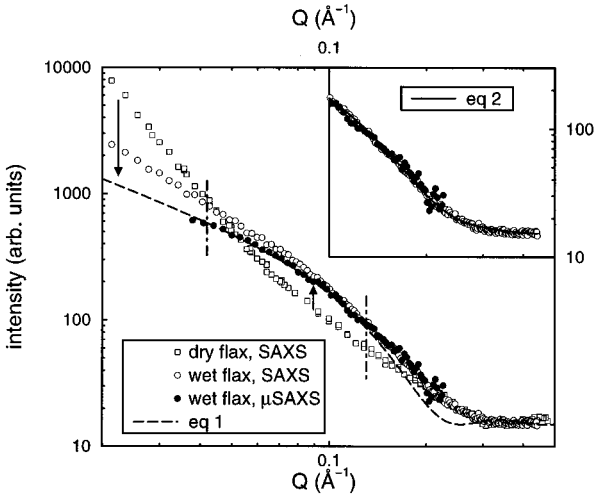

Figure 4. Spherical average of the two-dimensional μSAXS intensity (Figure 3), $\bar{I}(Q)$, displayed on a double-logarithmic scale (filled circles), and corresponding conventional SAXS curves of wet and dry flax fibers. The dashed line represents a fit with the model function from eq 1 for a monodisperse system (one single microfibril radius). The fit may be considerably improved by introducing a size distribution of the microfibril radii according to eq 2 (solid line in the inset). The down-arrow at low Q points out the reduction of pore scattering, the up-arrow at intermediate Q the enhancement of the SAXS signal by swelling the flax fibers with water. The dashed−dotted lines indicate the Q region of a straight line in a Guinier plot.

4.2. Microfibril Diameter. The further data analysis was based on the spherically averaged intensity $\bar{I}(Q)$ (see Experimental Details section). The scattering curve corresponding to the two-dimensional μSAXS pattern of Figure 3 (position $z = -4$ μm) is shown in Figure 4 (filled circles). It is compared to conventional SAXS measurements of dry (squares) and wet (open circles) flax fibers. The Q range of the latter experiments is larger as data measured at two different sample-detector distances were combined. In future μSAXS experiments, an enlargement of the Q range to higher Q may be achieved with a shorter sample−detector distance or, alternatively, with a larger X-ray wavelength. However, these changes were not possible in the framework of the experiment presented here.

There are marked differences between SAXS patterns of dry and wet fibers on the one hand and between SAXS and μSAXS data on the other hand. Effects in two separated Q regions have to be distinguished. First, as mentioned above, the swelling with water enhances the scattering contrast and, therefore, the small-angle intensity around $Q = 0.1$ Å^{-1} (Figure 4, up-arrow). Second, for fiber bundles (conventional experiment) the scattering contrast at the interface fiber−water or fiber−air causes additional intensity at small wave vector transfers ($Q \leq 0.09$ Å^{-1}). This pore scattering is reduced by water and it disappears completely for μSAXS as the interfaces are not illuminated (Figure 4, down-arrow). For $Q \geq 0.09$ Å^{-1} the SAXS and μSAXS data of wet fibers show perfect agreement.

The shape of cellulose microfibrils is well approximated by a cylinder. Assuming independent particle scattering in the water-swollen state[8] (this will be discussed below) the powder-averaged scattered intensity of cylindrical particles with radius r is given by[22,23]

$$\bar{I}(Q) = b + c\frac{r^4}{Q}\left(\frac{2J_1(Qr)}{Qr}\right)^2 \quad (1)$$

The addition of b accounts for a remaining constant background, c is a scaling constant, and J_1 denotes the Bessel function of first kind and first order. This model function was fitted to the data using a least-squares algorithm. However, as Figure 4 shows (dashed line), the simple model does not explain the measurements sufficiently. The mean radius can be determined to $r = 15$ Å, but for $Q \geq 0.12$ Å^{-1} the fitted curve begins to deviate from the data, showing a pronounced minimum at $Q \approx 0.23$ Å^{-1}. Such a minimum is a typical sign for a uniform particle size (monodispersity),[3] however, this kind of minimum ist not observed in the data. The problem may be solved by introducing a size distribution of microfibril radii. We chose a Gaussian with mean radius $\bar{r}$ and standard deviation σ_r. The model function in eq 1 is hence modified according to

$$\bar{I}(Q) = b + c\int_0^\infty \frac{r^4}{Q}\left(\frac{2J_1(Qr)}{Qr}\right)^2 \frac{1}{\sqrt{2\pi}\sigma_r} \exp\left(-\frac{(\bar{r}-r)^2}{2\sigma_r^2}\right) dr \quad (2)$$

The background parameter b was fixed to the value of the scattering intensity beyond $Q = 0.3$ Å^{-1} (see Figure 4). Thus, three parameters ($\bar{r}$, σ_r, and c) had to be determined in the fit. The best fit is shown in the inset of Figure 4 and corresponds to $\bar{r} = 9.4(4)$ Å and $\sigma_r = 4.8(3)$ Å. The smaller mean radius—with respect to the fit with eq 1—can be understood as follows: The scattered intensity of long cylinders depends on the square of their cross section (factor r^4 in eqs 1 and 2).[22] Thus, the contribution of larger microfibrils to $\bar{I}(Q)$ according to eq 2 is stronger than that of smaller ones. One can calculate that, in spite of the small mean radius, the integral in eq 2 is dominated by the scattering function of particles with $r' \approx 15.5$ Å. Thus, the fits with and without a size distribution function are not contradictory: The latter simply reveals the additional presence of smaller microfibrils.

A Guinier plot of the data—modified for cylindrical particles[22]—again is more sensitive to larger particles. It exhibits a straight line in the low-Q part (marked in Figure 4) where the slope consequently yields a mean radius of $\bar{r} \approx 15$ Å.

The microfibril diameter fitted to the data, 30(2) Å, corresponds well to the SAXS results of Heyn[8] who found 28 Å for flax as well as to transmission electron microscopy[6] (diameters ranging from 20 to 40 Å). However, both X-ray and neutron diffraction experiments[12] yielded considerably larger diameters for the crystalline microfibrils of ≈45 Å. Investigations of this discrepancy are under way. One possible reason is that the assumption of independent particle scattering is not valid even in the water-swollen state and that interparticle interference effects (due to mean lateral particle distances in the order of 50 Å) influence the SAXS signal.

Concerning the position (z) dependence of the microfibrils' size, the variation with z is rather small (average radius $\bar{r} = 15$ Å, standard deviation 1 Å). Also the general shape of the scattering curve—which may include interference effects, as stated above—does not show changes across the whole fiber diameter. In particular, there is no significant difference between the core and the skin of the fiber.

Finally, it is also noteworthy that the width of the distribution of microfibril diameters found here is considerably larger that in the cell wall of spruce wood. Indeed, a diameter of $2\bar{r} = 25$ Å and a distribution width of 4.4 Å (fwhm) were consistently found in spruce wood using SAXS, X-ray diffraction, and transmission electron microscopy.[3] This finding means that specific mechanisms of cell growth in different plants are related to the characteristics of the cellulose microfibrils in their cell walls, namely mean size and size distribution.

5. Conclusions

Small-angle X-ray scattering using a microfocus beam (μSAXS) was shown to provide unique information on the organization of cellulose microfibrils in a single flax fiber. Their orientation parallel to the fiber axis is nearly perfect with a distribution of tilt angles between ±3.5°. Furthermore, the fiber is built up homogeneously in the sense that mean diameter and spacing as well as tilt angle of the microfibrils are uniform over the whole fiber cross section. With respect to conventional SAXS, the intensity contribution from pore or surface scattering is completely avoided as the beam size is smaller than a single fiber. The microbeam will enable future SAXS investigations of microfibril arrangement in "kinks" of flax fibers (see Figure 1), which are known to differ in their mechanical properties from the straight fiber parts.

The μSAXS technique—as a position-resolved and very fast probe—will contribute to solving persisting problems concerning the supermolecular structure of cellulosic materials. Furthermore, the combination with fiber diffraction is easily possible without changing the sample. This enables the investigation of texture effects of the crystalline microfibrils in cell walls and fibers,[4,24] profiting from the microbeam in the same way as the SAXS experiments.

The present work has proven the feasibility to carry out position-resolved small-angle X-ray scattering experiments on thin biological samples in their native state, i.e., without any additional treatment as would be necessary for electron microscopy.

Acknowledgment. The authors wish to thank H. Chanzy (CERMAV-CNRS, Grenoble, France) for providing the sample and very fruitful discussions and R. Mezei (University of Budapest, Hungary) for her kind assistance in the Vienna SAXS experiment. The preparation of the electron micrograph (Figure 1) by I. Snigireva (ESRF) is greatfully acknowledged.

References and Notes

(1) Krässig, H. A. *Cellulose: Structure, Accessibility and Reactivity*; Polymer Monographs 11, Gordon and Breach Science Publishers: Yverdon, 1993.
(2) Sugiyama, J.; Vuong, R.; Chanzy, H. *Macromolecules* **1991**, *24*, 4168−4175.
(3) Jakob, H. F.; Fengel, D.; Tschegg, S. E.; Fratzl, P. *Macromolecules* **1995**, *28*, 8782−8787.
(4) Revol, J.-F. *Carbohydr. Polym.* **1982**, *2*, 123−134.
(5) Woodcock, C.; Sarko, A. *Macromolecules* **1980**, *13*, 1183−1187.
(6) Näslund, P.; Vuong, R.; Chanzy, H.; Jésior, J. C. *Text. Res. J.* **1988**, *58*, 414−417.
(7) Mary, M.; Revol, J.-F.; Goring, D. A. I. *J. Appl. Polym. Sci.* **1986**, *31*, 957−963.
(8) Heyn, A. N. J. *J. Appl. Phys.* **1955**, *26*, 519−526.
(9) Heyn, A. N. J. *J. Appl. Phys.* **1955**, *26*, 1113−1120.
(10) Haase, J.; Hosemann, R.; Renwanz, B. *Colloid Polym. Sci.* **1973**, *251*, 871−875.

(11) Haase, J.; Hosemann, R.; Renwanz, B. *Colloid Polym. Sci.* **1974**, *252*, 712−717.
(12) Müller, M.; Czihak, C.; Fratzl, P.; Vogl, G.; Schober, H.; Mezei, R.; Requardt, H. To be published.
(13) Riekel, C.; Cedola, A.; Heidelbach, F.; K. Wagner, K. *Macromolecules* **1997**, *30*, 1033−1037.
(14) Huang, T. C.; Toraya, H.; Blanton, T. H.; Wu, Y. *J. Appl. Crystallogr.* **1993**, *26*, 180−184.
(15) Waigh, T. A.; Hopkinson, I.; Donald, A. M.; Butler, M. F.; Heidelbach, F.; Riekel, C. *Macromolecules* **1997**, *30*, 3813−3820.
(16) Buléon, A.; Pontaire, B.; Riekel, C.; Chanzy, H.; Helbert, W.; Vuong, R. *Macromolecules* **1997**, *30*, 3952−3954.
(17) Hammersley, A. P.; Svensson, S. O.; Thompson, A. *Nucl. Instrum. Methods A* **1994**, *346*, 312−321.
(18) The microfibril arrangement has cylindrical symmetry. Therefore, a spherical average corresponds to an azimuthal average of the two-dimensional data weighted with $\sin(\varphi)$, where φ is the azimuthal angle. We left out the multiplication with $\sin(\varphi)$ since the respective correction to $\bar{I}(Q)$ could be shown to be within the statistical error in the Q range analyzed here.
(19) Porod, G. *Fortschr. Hochpolym.-Forsch.* **1961**, *2*, 363−400.
(20) Fischer, E. W.; Herchenröder, P.; Manley, R. St.; Stamm, M. *Macromolecules* **1978**, *11*, 213−217.
(21) Hentschel, M. P.; Hosemann, R.; Lange, A.; Uther, B.; Brückner, R. *Acta Crystallogr. A* **1987**, *43*, 506−513.
(22) Glatter, O., Kratky, O., Eds.; *Small-angle X-Ray Scattering*; Academic Press: New York, 1982.
(23) Jakob, H. F.; Tschegg, S. E.; Fratzl, P. *Macromolecules* **1996**, *29*, 8435−8440.
(24) Revol, J.-F.; Gancet, C.; Goring, D. A. I. *Wood Sci.* **1982**, *14*, 120−126.

MA980004C